



Discover Generics

Cost-Effective CT & MRI Contrast Agents

 FRESENIUS
KABI

[WATCH VIDEO](#)

AJNR

This information is current as
of June 29, 2025.

Diagnostic Performance of Whole-Body Ultra-Low-Dose CT for Detection of Mechanical Ventriculoperitoneal Shunt Complications: A Retrospective Analysis










S. Afat, R. Pjontek, O. Nikoubashman, W.G. Kunz, M.A.
Brockmann, H. Ridwan, M. Wiesmann, H. Clusmann, A.E.
Othman and H.A. Hamou

AJNR Am J Neuroradiol 2022, 43 (11) 1597-1602

doi: <https://doi.org/10.3174/ajnr.A7672>

<http://www.ajnr.org/content/43/11/1597>

Diagnostic Performance of Whole-Body Ultra-Low-Dose CT for Detection of Mechanical Ventriculoperitoneal Shunt Complications: A Retrospective Analysis

 S. Afat,  R. Pjontek,  O. Nikoubashman,  W.G. Kunz, M.A. Brockmann,  H. Ridwan,  M. Wiesmann,  H. Clusmann,  A.E. Othman, and  H.A. Hamou



ABSTRACT

BACKGROUND AND PURPOSE: Radiographic shunt series are still the imaging technique of choice for radiologic evaluation of VP-shunt complications. Radiographic shunt series are associated with high radiation exposure and have a low diagnostic performance. Our aim was to investigate the diagnostic performance of whole-body ultra-low-dose CT for detecting mechanical ventriculoperitoneal shunt complications.

MATERIALS AND METHODS: This retrospective study included 186 patients (mean age, 54.8 years) who underwent whole-body ultra-low-dose CT (100 kV[peak]; reference, 10 mAs). Two radiologists reviewed the images for the presence of ventriculoperitoneal shunt complications, image quality, and diagnostic confidence. On a 5-point Likert scale, readers scored image quality and diagnostic confidence (1 = very low, 5 = very high). Sensitivity, specificity, positive predictive value, and negative predictive value were calculated. Radiation dose estimation of whole-body ultra-low-dose CT was calculated and compared with the radiation dose of a radiographic shunt series.

RESULTS: 34 patients positive for VP-shunt complications were correctly identified on whole-body ultra-low-dose CT by both readers. No false-positive or -negative cases were recorded by any of the readers, yielding a sensitivity of 100% (95% CI, 87.3%–100%), a specificity of 100% (95% CI, 96.9%–100%), and perfect agreement ($\kappa = 1$). Positive and negative predictive values were high at 100%. Shunt-specific image quality and diagnostic confidence were very high (median score, 5; range, 5–5). Interobserver agreement was substantial for image quality ($\kappa = 0.73$) and diagnostic confidence ($\kappa = 0.78$). The mean radiation dose of whole-body ultra-low-dose CT was significantly lower than the radiation dose of a conventional radiographic shunt series (0.67 [SD, 0.4] mSv versus 1.57 [SD, 0.6] mSv; 95% CI, 0.79–1.0 mSv; $P < .001$).

CONCLUSIONS: Whole-body ultra-low-dose CT allows detection of ventriculoperitoneal shunt complications with excellent diagnostic accuracy and diagnostic confidence. With concomitant radiation dose reduction on contemporary CT scanners, whole-body ultra-low-dose CT should be considered an alternative to the radiographic shunt series.

ABBREVIATIONS: IQR = interquartile range; VP-shunt = ventriculoperitoneal shunt; WB-ULD-CT = whole-body ultra-low-dose CT

Hydrocephalus is a common, surgically treatable disorder, defined as a pathologic accumulation of CSF resulting in a serious expansion of the brain ventricles. Ventriculoperitoneal

shunt (VP-shunt) is an effective treatment for hydrocephalus. VP-shunts drain the excess CSF into the peritoneum, where it can be absorbed.^{1–3} However, VP-shunts have a high complication rate of 20%–40% within the first year of placement.^{4–8} The clinical symptoms of VP-shunt complications can vary and are often not specific. Errors in diagnosis can have serious consequences for patients. Thus, imaging is the primary method to detect VP-shunt complications.⁹

Radiographic shunt series are still the imaging technique of choice for radiologic evaluation of VP-shunt complications.¹⁰ Shunt series cover the whole course of VP-shunts from the head to abdomen and usually consist of frontal skull, lateral skull, frontal chest, frontal abdomen, and lateral abdomen radiographs. However, recent studies on the diagnostic performance of radiographic shunt series reported remarkably low sensitivities (between 8.3% and 31%)

Received June 21, 2022; accepted after revision September 7.

From the Department for Diagnostic and Interventional Radiology (S.A., A.E.O.), University Hospital Tuebingen, Tuebingen, Germany; Departments of Neurosurgery (R.P., H.C., H.A.H.) and Diagnostic and Interventional Neuroradiology (O.N., H.R., M.W.), University Hospital RWTH Aachen, Aachen, Germany; Department of Radiology (W.G.K.), University Hospital Ludwig-Maximilians-University, Munich, Germany; and Department of Neuroradiology (M.A.B., A.E.O.), University Medical Center of the Johannes Gutenberg University Mainz, Mainz, Germany.

Please address correspondence to Ahmed Othman, MD, University Medical Center Mainz, Department of Neuroradiology, Langenbeckstr 1, 55131 Mainz, Germany; e-mail: ahmed.e.othman@googlemail.com; @Afatdr

<http://dx.doi.org/10.3174/ajnr.A7672>

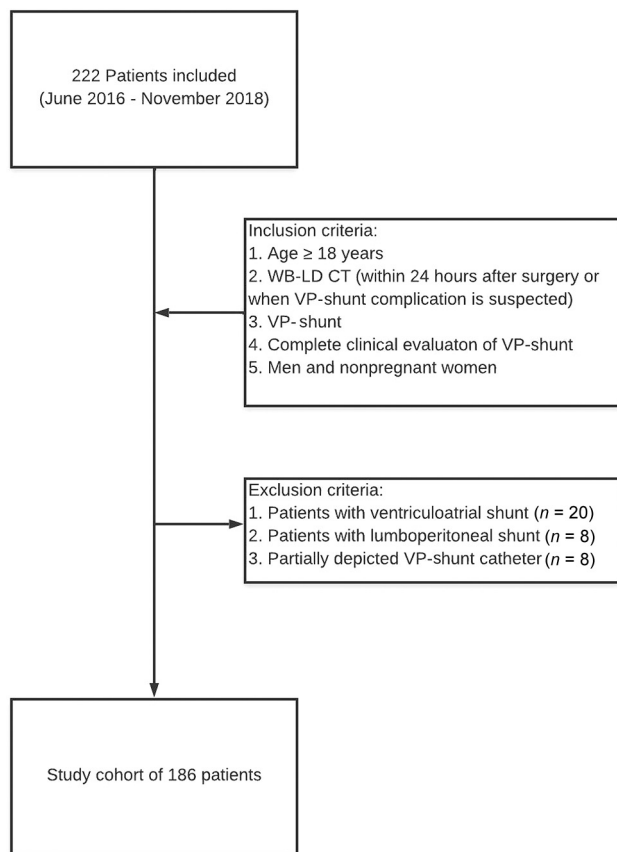


FIG 1. Standards for Reporting of Diagnostic Accuracy flow chart of patient inclusion.

to detect mechanical VP-shunt complications.¹¹⁻¹⁵ Radiographic shunt series often do not provide precise information about the abdominal catheter position. This leads to repeat x-ray examinations or even an additional (full-dose) CT.

Furthermore, radiographic shunt series are associated with high radiation exposure.¹⁴ Due to the low sensitivity and high radiation exposure, better imaging alternatives are necessary. CT is usually associated with considerably higher radiation doses than radiographs. However, the radiation dose of CT protocols can be adapted to the clinical question. For example, in case of VP-shunts, the radiation dose can be remarkably reduced while the hyperdense shunt catheters can easily be visualized despite high image noise. Recent animal studies have shown that whole-body ultra-low-dose CT (WB-ULD-CT) with radiation doses lower than those in the radiographic shunt series visualizes the VP-shunt properly and enables detection of VP-shunt complications with higher accuracy than radiographic images.^{16,17}

Nonetheless, human studies are necessary to evaluate these promising findings. On the basis of experimental findings, ULD-CT protocols for VP-shunt imaging have been implemented into the clinical routine at various centers. Pala et al¹⁸ compared WB-ULD-CT with radiography and showed that ULD-CT allows significantly better visualization of the distal catheter using a lower radiation dose than a radiographic shunt series. We hypothesize that WB-ULD-CT for assessment of VP-shunt complications in humans is feasible and can be

attained with high diagnostic accuracy and lower radiation doses than a radiographic shunt series. In the present study, we aimed to evaluate the diagnostic accuracy of WB-ULD-CT, focusing on the detection of mechanical VP-shunt malfunctions with an even lower radiation dose.

MATERIALS AND METHODS

Our local institutional ethics committee of the University of Aachen, Germany, approved this retrospective study and waived informed patient consent (registration number: EK 219/19).

Study Population

As a consequence of encouraging animal model results, we replaced the conventional radiographic shunt series with WB-ULD-CT for VP-shunt imaging in our institution by June 2016. As in many neurosurgical departments, VP-shunt imaging is performed routinely within 24 hours after implantation to ensure and precisely document the correct placement and verify the postprocedural course of the VP-shunt catheter. VP-shunt imaging is also performed when complications are suspected.

The inclusion period of this retrospective analysis was between June 2016 and November 2018. A total of 222 patients with VP-shunts underwent WB-ULD-CT during the inclusion period. The inclusion criteria for our study were the following: 1) 18 years of age or older, 2) WB-ULD-CT (within 24 hours after implantation of a VP-shunt or when VP-shunt failure was suspected), 3) VP-shunt, 4) complete clinical evaluation of the VP-shunt (including operative assessment if necessary), and 5) men and nonpregnant women. Patients with incomplete imaging of the course of the VP-shunt were excluded. The final sample size consisted of 186 patients; a Standards for Reporting of Diagnostic Accuracy flow chart of patient inclusion is shown in Fig 1.

Age, sex, etiology of hydrocephalus, history of a previous VP-shunt complication, the presence of symptoms, and operative/clinical results were recorded.

Imaging Technique and CT Image Reconstruction

All patients underwent WB-ULD-CT on a 40-section CT scanner (Somatom Definition AS; Siemens). The x-ray tube was operated at a tube voltage of 100 kV(peak) and a reference tube current of 10 mAs (collimation = 40 × 0.6 mm, pitch = 1.5). Automatic attenuation-based tube-current modulation (CARE Dose4D; Siemens) was activated. All reconstructions were acquired using a kernel (B45) with 5-mm (3-mm increment) section thickness and 1 mm (1-mm increment) in the axial, coronal, and sagittal planes. Images were generated using iterative reconstruction (Sinogram Affirmed Iterative Reconstruction Strength 3).

Moreover, 3D reconstructions using a volume-rendering technique were created.

Reference Standard

A neurosurgeon (H.A.H.) with 10 years of experience evaluated all patients' clinical data, including symptoms, clinical examinations, intraoperative findings, and recorded readmissions and VP-shunt revisions for a 3-month period after WB-ULD-CT imaging. Patients were classified as negative when clinical and operative work-up revealed no VP-shunt complications and

Table 1: Patient characteristics

Characteristic	Value
Sex	
Male	85/186 (45%)
Female	101/186 (54%)
Overall age (range) (yr)	54.8 (18–88)
Underlying etiology	
Tumor	12/186 (6%)
Posthemorrhagic hydrocephalus	59/186 (31%)
Congenital hydrocephalus	16/186 (8%)
Postinfectious hydrocephalus	5/186 (2%)
Posttraumatic hydrocephalus	12/186 (6%)
Posterior fossa cyst	2/186 (1%)
Idiopathic intracranial hypertension	23/186 (12%)
Normal-pressure hydrocephalus	40/186 (46%)
Aqueduct stenosis	17/186 (9%)
Symptoms	
Yes	
Headache	33/186 (17%)
Nausea and vomiting	9/186 (4%)
Fatigue	19/186 (10%)
Gait disturbance	34/186 (18%)
Others	36/186 (19%)
Multiple	5/186 (2%)
No	50/186 (26%)
Clinical indication	
24 Hours after implantation	102/186 (54%)
Complication suspected	84/186 (45%)
Secondary findings	
Dyslectasis	7/186 (3%)
Pneumonia	2/186 (1%)
Pleural effusion	6/186 (3%)
Nephrolithiasis	1/186 (0,5%)
Incidental tumor findings	1/186 (0,5%)
Abdominal aortic aneurysm	1/186 (0,5%)

when no VP-shunt-related readmissions were recorded within the 3-month period after imaging. Patients were classified as positive when mechanical VP-shunt complications were identified in the clinical examination and intraoperatively.

Image Evaluation

Image evaluation was performed on a standard PACS workstation. After the definition of the reference standard, 2 radiologists (A.E.O. with 8 years of experience; S.A. with 6 years of experience) who were blinded to all clinical data, independently evaluated WB-ULD-CT reconstructions regarding shunt-specific overall image quality and diagnostic confidence using 5-point Likert scales (1, very low; 5, excellent).¹⁹ The same readers assessed the WB-ULD-CT images regarding the presence/absence and type of mechanical shunt complication.

Radiation Dose Estimation

The dose-length product was obtained and used to estimate the effective radiation dose for all patients. The effective dose was estimated by multiplying the dose-length product by $0.015 \text{ mSv} \times \text{mGy}^{-1} \times \text{cm}^{-1}$ (conversion factor).^{20,21}

Statistical Analysis

Statistical analyses were performed using SPSS Statistics for Windows 25 (IBM). The mean accounted effective dose for WB-ULD-CT was then compared with the reported cumulative

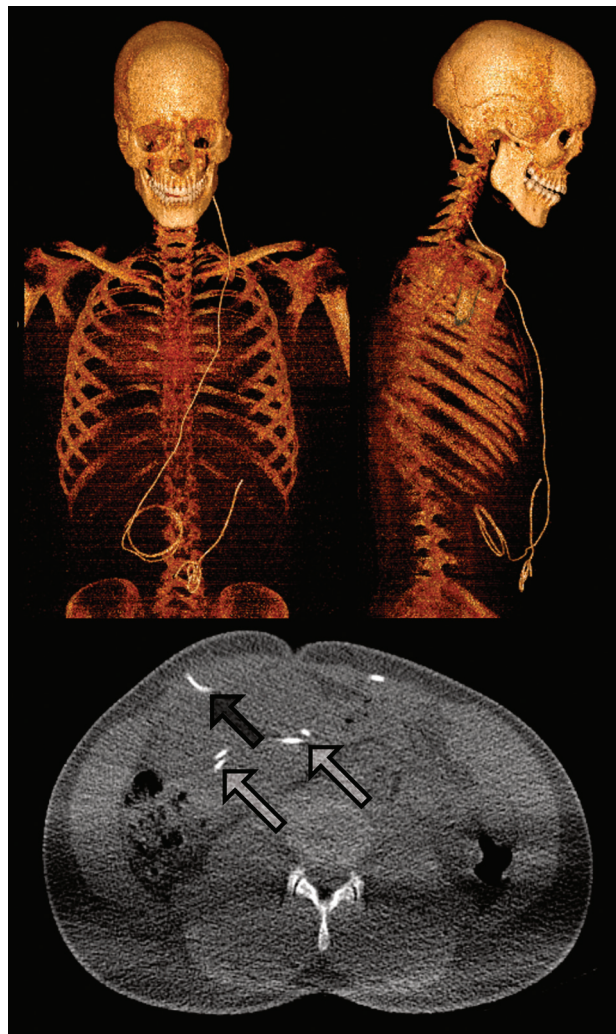


FIG 2. As a premature infant, a 19-year-old man developed intraventricular hemorrhage grade IV with consecutive posthemorrhagic hydrocephalus and formation of a left frontal intracranial cyst. A cysto-ventriculoperitoneal shunt was implanted during the first months of life. At 19 years of age, the patient was referred to our center because of abdominal pain and local induration around the right abdominal scar. WB-ULD-CT revealed an intraperitoneal position of the distal catheter, however with an intraperitoneal cyst or pseudocyst formation. Front (upper left) and lateral (upper right) views of the 3D reconstruction show looping of the peritoneal catheter. On the axial conformation with 5-mm section thickness, intraperitoneal insertion of the catheter (full arrow) as well as intraperitoneal pseudocyst with incorporated catheter loops (transparent arrows) can be detected.

radiation exposure by Shuaib et al¹⁴ of 1.57 (SD, 0.6) mSv per shunt series by calculating the difference between the 2 means, the significance value (*P* value), and the 95% CI. Overall image quality and diagnostic confidence were expressed as median and interquartile range (IQR) of both readers. Sensitivity, specificity, positive predictive value, negative predictive value, and diagnostic accuracy of WB-ULD-CT with 95% CIs were calculated for the detection of mechanical VP-shunt complications on WB-ULD-CT using the above-mentioned reference standard. The Cohen κ coefficient was calculated for interrater agreement. A *P* value was considered significant at *P* < .05.

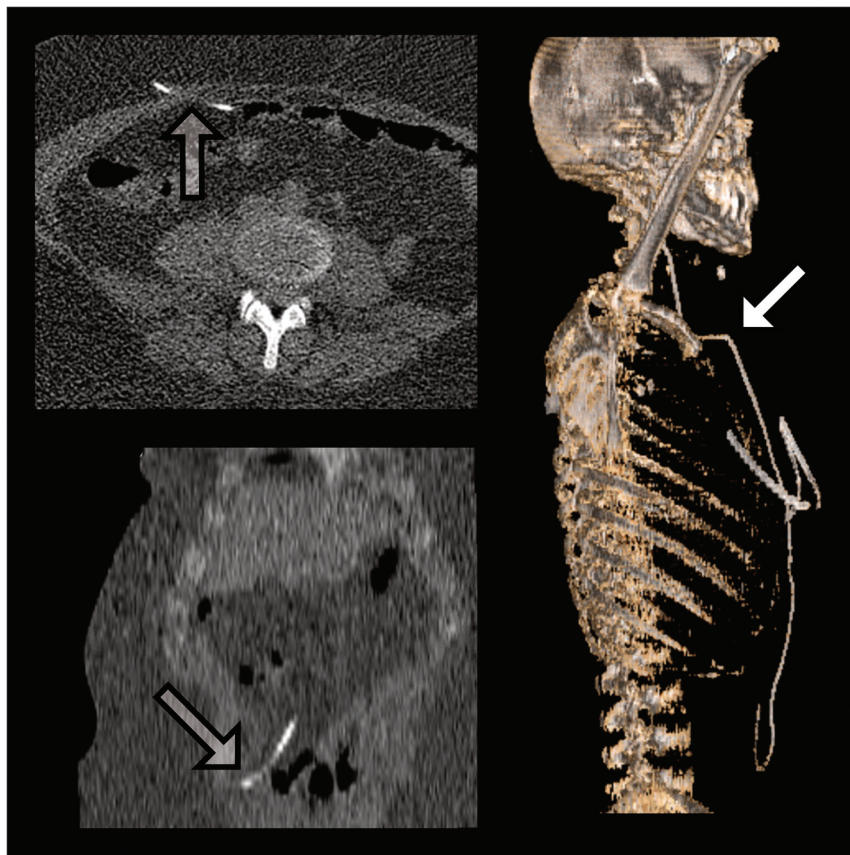


FIG 3. A 33-year-old woman presented with progressive headache, nausea, and vomiting, indicating a shunt dysfunction. Several shunt revisions were needed during infancy. The 3D reconstruction of the current WD-ULD-CT (right) depicts kinking of the shunt tube at the right clavicle (white arrow) as well as short distal catheter in relation to an adult body size. However, the distal catheter passed through the peritoneum (transparent arrows on axial and coronal reconstructions on the left) and ends intraperitoneally.

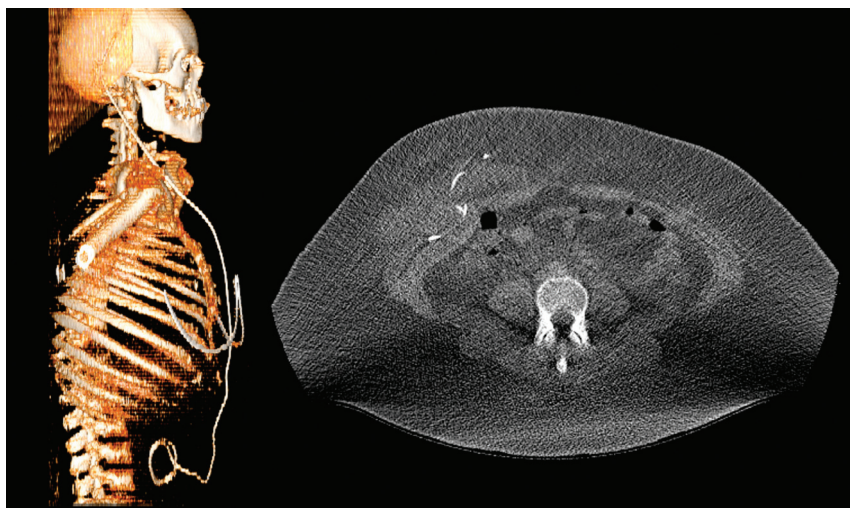


FIG 4. A 26-year-old woman with obesity (body mass index, 35.3 kg/m²) with idiopathic intracranial hypertension received a VP-shunt after the failure of conservative therapy. After the implantation of a VP-shunt, the correct intraperitoneal position of the distal catheter was verified by WB-ULD-CT. Two weeks later she was admitted due to progressive abdominal pain. WB-ULD-CT (lateral view on 3D reconstruction on the left and axial reconstruction on the right) shows an extraperitoneal shunt dislocation.

RESULTS

Patient Characteristics

The study cohort consisted of 186 patients (mean age, 54.8 years; range, 18–88 years), including 85 men (45.7%; mean age, 58.5 years; range, 19–87 years) and 101 women (54.3%; mean age, 51.6 years; range, 18–88 years); 54.8% of the WB-ULD-CT studies were within 24 hours after implantation of a new VP-shunt; and 45.2% of the WB-ULD-CT studies were performed when shunt failure was suspected. Further patient characteristics are given in Table 1.

Diagnostic Evaluation

Of the 186 patients, 152 patients (81.7%) were negative for mechanical complications. Thirty-four patients (18.3%) had VP-shunt complications. Seven patients (3.8%) had a breakage/disconnection of the subcutaneous shunt catheter, 1 patient had an abdominal pseudocyst (0.5%) (Fig 2) at the tip of the catheter, 2 patients (1.1%) had kinking of the catheter (Fig 3), and 24 patients (12.9%) (Fig 4) had a dislocation of the distal/peritoneal VP-shunt catheter (Table 2).

Both readers detected all 34 complications (18.3%) of 186 patients with a perfect agreement ($\kappa = 1$). There were no patients with false-negative or false-positive findings, resulting in a sensitivity of 100% (95% CI, 87.3%–100%) and a specificity of 100% (95% CI, 96.9%–100%). WB-ULD-CT showed a high positive predictive value of 100% (95% CI, 87.3%–100%) and a high negative predictive value of 100% (95% CI, 96.9%–100%).

Overall Image Quality and Diagnostic Confidence

The overall shunt-specific image quality was rated very high by both readers, with a mean score of 5 (IQR, 25%–75%; range, 5–5) and substantial interrater agreement ($\kappa \geq 0.73$). The diagnostic confidence of both readers was rated very high with a median score of 5 (IQR, 25%–75%; range, 5–5), and a substantial interrater agreement ($\kappa \geq 0.78$).

Radiation Dose Estimation

The mean dose-length product of WB-ULD-CTs was 45.04 (SD, 26.91) mGy ×

Table 2: Overview of detected shunt complications in WB-LD-CT by 2 readers (A.E.O. and S.A.)

Complication Type	Reader A	Reader B
Disconnection	7/7 (100%)	7/7 (100%)
Dislocation	24/24 (100%)	24/24 (100%)
Kinking	2/2 (100%)	2/2 (100%)
Pseudocyst	1/1 (100%)	1/1 (100%)
Total	34/34 (100%)	34/34 (100%)

cm (minimum, 12 mGy × cm; maximum, 225 mGy × cm), resulting in a mean estimated effective radiation dose of 0.67 (SD, 0.4) mSv (minimum, 0.18 mSv; maximum, 3.37 mSv). The mean radiation dose of WB-ULD-CT was significantly lower than the radiation dose of the radiographic shunt series as reported by Shuaib et al¹⁴ (0.67 [SD, 0.4] mSv versus 1.57 [SD, 0.6] mSv; 95% CI, 0.79–1.0 mSv; $P < .001$).

DISCUSSION

Imaging plays an essential role in the clinical work-up of adult patients with suspected VP-shunt complications or in postprocedural diagnostics. In daily practice, suspicion of VP-shunt complications is mostly confirmed on the basis of the combination of imaging findings and clinical work-up. In the present work, we evaluated radiation exposure and diagnostic performance of WB-ULD-CT for the detection of mechanical VP-shunt complications, and this study is currently the largest cohort of patients with VP-shunts who underwent WB-ULD-CT.

Our findings indicate that WB-ULD-CT has a high diagnostic accuracy for the detection of mechanical VP-shunt complications with a lower radiation dose than in radiographic shunt series.

Despite the restricted radiation dose of WB-ULD-CT, VP-shunt catheters could be appropriately visualized with sufficient image quality and diagnostic confidence. The readers were able to detect all 34 VP-shunt complications correctly without producing false-positive or false-negative findings.

Other studies, such as the one by Lehnert et al,¹² showed a poor sensitivity of a radiographic shunt series for the detection of mechanical complications (sensitivity = 4%), which resulted in no significant impact on patient outcome regarding surgical shunt revision (OR, 0.9; 95% CI, 0.7–1.2; $P = .74$). A further study also reported the poor sensitivity of a radiographic shunt series for the detection of VP-shunt complications (sensitivity = 31%).¹¹

On the other hand, animal studies have shown that WB-ULD-CT is remarkably superior to a radiographic shunt series for the detection of mechanical VP-shunt complications.^{16,17,22} Especially, extraperitoneal dislocation, which can easily be missed on a radiographic shunt series, is easy to detect on CT images.

Our results have the potential to make WB-ULD-CT the criterion standard of diagnostic imaging of VP-shunts because many neurosurgical centers perform radiographic shunt series and non-contrast-enhanced CT of the head in the early postoperative phase as a routine procedure after implanting new hardware in the body of the patient and to detect postoperative complications if suspected.¹⁰

In addition, our study supports previous studies showing a significantly lower radiation dose compared with a radiologic

shunt series, even though in our study, the comparison was not intraindividual.^{11,12,16,17,22}

The observed high diagnostic accuracy of WB-ULD-CT for the detection of VP-shunt complications in our study emphasizes the potential role of WB-ULD-CT as an alternative to plain radiographs for VP-shunt imaging.

In a retrospective study by Pala et al,¹⁸ the low-dose CT had a lower radiation exposure than the x-ray series. However, the mean radiation exposure was higher than in our study (0.67 mSv versus 1.9 mSv). Also, another strength of our study is the size of the cohort, which is larger than the cohort of Pala et al.

We believe that WB-ULD-CT is more applicable for routine clinical practice because it is a time-saving, one-stop-shop method with high diagnostic accuracy and a reduced radiation dose compared with a radiographic series.¹⁴ Patients are not repositioned several times as is the case with x-ray examinations when several regions of the body must be examined. Instead, they are placed on the CT table only once, and the examination is performed from the entire shunt course. This approach is of great importance, especially postoperatively or in patients requiring intensive care.

We believe that the radiation dose could even be further reduced and image quality improved by using new technologies like advanced new iterative reconstruction, new filtering techniques, dual-energy CT, modern radiography hardware, and artificial intelligence-based reconstruction techniques.^{23,24}

The retrospective single-center design of this study is a limitation. A multicenter approach with a larger cohort is required to reconfirm the results of our study. Due to the retrospective nature of the study, it was not possible to perform an interpatient comparison of performance and radiation dose between WB-ULD-CT and a conventional radiographic shunt series.

CONCLUSIONS

Our retrospective study indicates that WB-ULD-CT yields a high diagnostic accuracy for the detection of VP-shunt complications. Therefore, we believe that WB-ULD-CT is the first stage in the further development of the WB-ULD-CT protocol to replace radiologic shunt series as the new criterion standard.

Ethics Approval

Institutional Review Board approval was obtained from the University of Aachen before the initiation of this study.

Disclosure forms provided by the authors are available with the full text and PDF of this article at www.ajnr.org.

REFERENCES

1. Little AS, Zabramski JM, Peterson M, et al. **Ventriculoperitoneal shunting after aneurysmal subarachnoid hemorrhage: analysis of the indications, complications, and outcome with a focus on patients with borderline ventriculomegaly.** *Neurosurgery* 2008;62:618–27; discussion 618–27 [CrossRef Medline](#)
2. Hoh BL, Kleinhenz DT, Chi YY, et al. **Incidence of ventricular shunt placement for hydrocephalus with clipping versus coiling for ruptured and unruptured cerebral aneurysms in the Nationwide Inpatient Sample database: 2002 to 2007.** *World Neurosurg* 2011;76:548–54 [CrossRef Medline](#)

3. Brean A, Eide PK. **Prevalence of probable idiopathic normal pressure hydrocephalus in a Norwegian population.** *Acta Neurol Scand* 2008;118:48–53 [CrossRef Medline](#)
4. Al-Tamimi YZ, Sinha P, Chumas PD, et al; British Pediatric Neurosurgery Group Audit Committee. **Ventriculoperitoneal shunt 30-day failure rate: a retrospective international cohort study.** *Neurosurgery* 2014;74:29–34 [CrossRef Medline](#)
5. Farahmand D, Hilmarsson H, Hogfeldt M, et al. **Perioperative risk factors for short term shunt revisions in adult hydrocephalus patients.** *J Neurol Neurosurg Psychiatry* 2009;80:1248–53 [CrossRef Medline](#)
6. Park MK, Kim M, Park KS, et al. **A retrospective analysis of ventriculoperitoneal shunt revision cases of a single institute.** *J Korean Neurosurg Soc* 2015;57:359–63 [CrossRef Medline](#)
7. Reddy GK, Bollam P, Caldito G. **Long-term outcomes of ventriculoperitoneal shunt surgery in patients with hydrocephalus.** *World Neurosurg* 2014;81:404–10 [CrossRef Medline](#)
8. Barton SE, Campbell JW, Piatt JH. **Quality measures for the management of hydrocephalus: concepts, simulations, and preliminary field-testing.** *J Neurosurg Pediatr* 2013;11:392–97 [CrossRef Medline](#)
9. Lee MJ, Streicher DA, Howard BM, et al. **Ventricular shunt radiographs: still relevant in the cross-sectional era? Pictorial review of the radiographic appearance of ventricular shunts and approach to interpreting shunt series radiographs.** *Neurographics* 2016;6:202–12 [CrossRef](#)
10. Kamenova M, Rychen J, Guzman R, et al. **Yield of early postoperative computed tomography after frontal ventriculoperitoneal shunt placement.** *PLoS One* 2018;13:e0198752 [CrossRef Medline](#)
11. Desai KR, Babb JS, Amodio JB. **The utility of the plain radiograph “shunt series” in the evaluation of suspected ventriculoperitoneal shunt failure in pediatric patients.** *Pediatr Radiol* 2007;37:452–56 [CrossRef Medline](#)
12. Lehnert BE, Rahbar H, Relyea-Chew A, et al. **Detection of ventricular shunt malfunction in the ED: relative utility of radiography, CT, and nuclear imaging.** *Emerg Radiol* 2011;18:299–305 [CrossRef Medline](#)
13. Griffey RT, Ledbetter S, Khorasani R. **Yield and utility of radiographic “shunt series” in the evaluation of ventriculo-peritoneal shunt malfunction in adult emergency patients.** *Emerg Radiol* 2007;13:307–11 [CrossRef Medline](#)
14. Shuaib W, Johnson JO, Pande V, et al. **Ventriculoperitoneal shunt malfunction: cumulative effect of cost, radiation, and turnaround time on the patient and the health care system.** *AJR Am J Roentgenol* 2014;202:13–17 [CrossRef Medline](#)
15. Pujara S, Natalwala A, Robertson I. **Referrals for suspected ventriculo-peritoneal shunt dysfunction and necessity for further imaging.** *Br J Neurosurg* 2017;31:320–21 [CrossRef Medline](#)
16. Afat S, Pjontek R, Hamou HA, et al. **Imaging of ventriculoperitoneal shunt complications: comparison of whole-body low-dose computed tomography and radiographic shunt series.** *J Comput Assist Tomogr* 2016;40:991–96 [CrossRef Medline](#)
17. Othman A, Hamou HA, Pjontek R, et al. **Evaluation of whole body ultralow-dose CT for the assessment of ventriculoperitoneal shunt complications: an experimental ex-vivo study in a swine model.** *Eur Radiol* 2015;25:2199–2204 [CrossRef Medline](#)
18. Pala A, Awad F, Braun M, et al. **Value of whole-body low-dose computed tomography in patients with ventriculoperitoneal shunts: a retrospective study.** *J Neurosurg* 2018;129:1598–1603 [CrossRef Medline](#)
19. Notohamiprodjo S, Stahl R, Braunagel M, et al. **Diagnostic accuracy of contemporary multidetector computed tomography (MDCT) for the detection of lumbar disc herniation.** *Eur Radiol* 2017;27:3443–51 [CrossRef Medline](#)
20. Christner JA, Kofler JM, McCollough CH. **Estimating effective dose for CT using dose-length product compared with using organ doses: consequences of adopting International Commission on Radiological Protection publication 103 or dual-energy scanning.** *AJR Am J Roentgenol* 2010;194:881–89 [CrossRef Medline](#)
21. American Association of Physicists in Medicine Task Group 23. **The Measurement, Reporting, and Management of Radiation Dose in CT.** American Association of Physicists in Medicine; 2008 [CrossRef](#)
22. Othman AE, Afat S, Hamou HA, et al. **High-pitch low-dose whole-body computed tomography for the assessment of ventriculoperitoneal shunts in a pediatric patient model: an experimental ex vivo study in rabbits.** *Invest Radiol* 2015;50:858–62 [CrossRef Medline](#)
23. Abdi AJ, Mussmann B, Mackenzie A, et al. **Visual evaluation of image quality of a low dose 2D/3D slot scanner imaging system compared to two conventional digital radiography x-ray imaging systems.** *Diagnostics (Basel)* 2021;11:1932 [CrossRef Medline](#)
24. Monuszko K, Malinzak M, Yang LZ, et al. **Image quality of EOS low-dose radiography in comparison with conventional radiography for assessment of ventriculoperitoneal shunt integrity.** *J Neurosurg Pediatr* 2021;27:375–81 [CrossRef Medline](#)